THESIS FOR THE DEGREE OF DOCTOR OF PHILOSOPHY

Force-based control for human-robot cooperative object manipulation

Ramin Jaberzadeh Ansari

CHALMERS
UNIVERSITY OF TECHNOLOGY

Department of Electrical Engineering
Chalmers University of Technology
Göteborg, Sweden, 2021

Force-based control for human-robot cooperative object manipulation
Ramin Jaberzadeh Ansari
ISBN 978-91-7905-515-8

© Ramin Jaberzadeh Ansari, 2021.

Doktorsavhandlingar vid Chalmers tekniska högskola
Ny serie nr 4982
ISSN 0346-718X

Department of Electrical Engineering
Chalmers University of Technology
SE-412 96 Göteborg, Sweden
Telephone: +46 (0)31 772 1000
`www.chalmers.se`

Typeset by the author using LaTeX.

Printed by Chalmers Reproservice
Göteborg, Sweden, May 2021

To my family

Abstract

In Physical Human-Robot Interaction (PHRI), humans and robots share the workspace and physically interact and collaborate to perform a common task. However, robots do not have human levels of intelligence or the capacity to adapt in performing collaborative tasks. Moreover, the presence of humans in the vicinity of the robot requires ensuring their safety, both in terms of software and hardware. One of the aspects related to safety is the stability of the human-robot control system, which can be placed in jeopardy due to several factors such as internal time delays. Another aspect is the mutual understanding between humans and robots to prevent conflicts in performing a task. The kinesthetic transmission of the human intention is, in general, ambiguous when an object is involved, and the robot cannot distinguish the human intention to rotate from the intention to translate (the translation/rotation problem).

This thesis examines the aforementioned issues related to PHRI. First, the instability arising due to a time delay is addressed. For this purpose, the time delay in the system is modeled with the exponential function, and the effect of system parameters on the stability of the interaction is examined analytically. The proposed method is compared with the state-of-the-art criteria used to study the stability of PHRI systems with similar setups and high human stiffness. Second, the unknown human grasp position is estimated by exploiting the interaction forces measured by a force/torque sensor at the robot end effector. To address cases where the human interaction torque is non-zero, the unknown parameter vector is augmented to include the human-applied torque. The proposed method is also compared via experimental studies with the conventional method, which assumes a contact point (i.e., that human torque is equal to zero). Finally, the translation/rotation problem in shared object manipulation is tackled by proposing and developing a new control scheme based on the identification of the ongoing task and the adaptation of the robot's role, i.e., whether it is a passive follower or an active assistant. This scheme allows the human to transport the object independently in all degrees of freedom and also reduces human effort, which is an important factor in PHRI, especially for repetitive tasks. Simulation and experimental results clearly demonstrate that the force required to be applied by the human is significantly reduced once the task is identified.

Keywords: physical human-robot collaboration, kinesthetic perception, human-robot interaction control, system identification

Acknowledgments

First of all, I would like to thank my supervisor Yiannis Karayiannidis for giving me the opportunity to work on an exciting and challenging topic. Thanks for all the fruitful discussions and continuous encouragement. I would also like to thank my co-supervisor Jonas Sjöberg. I appreciate your valuable guidance.

I am thankful to my colleagues at the Division of Systems and Control. In particular, I would like to thank my office mate Ankit for all the good times, interesting conversations and his friendship. I would also like to show my appreciation to Giuseppe for the technical discussions when I needed them. I would like to thank Albin and Rita for nice conversations during our group meetings. Muddassar, Elena, Endre, Ivo, Angelos, Robert, Simon, Fredrik, Anton and Nalin thank you for contributing to a fantastic work environment. I am also thankful to everyone at the Electrical Engineering Department for making Chalmers an excellent workplace for me. In addition, I would like to acknowledge my colleagues at Volvo Trucks, especially Per-Lage Götvall, for inspiring me in the early stages of this research.

To all my Iranian friends, in particular: Abolfazl, Ahad, Alireza, Bita, Ebrahim, Fatemeh, Kamran, Maliheh, Masoud, Mohammad Ali, Navid, Parastoo, Pegah, Sadegh, Taha, and Zahra, thank you for all parties, activities, and fikas which gave me a good work-life balance during my study. Many thanks go to my friends, Abbas, Astrid, Sepideh, and Sina for making lots of memorable and happy days and always being a major source of support and kindness.

My deep and sincere gratitude to my family, especially my parents, for their continuous and unparalleled love, help, and support. Finally, I would like to thank Samar for her endless support and love, and for being my dearest companion.

Ramin Jaberzadeh Ansari
Göteborg, Sweden, May 2021

List of Publications

This thesis is based on the following appended publications:

[A] **R. Jaberzadeh Ansari**, J. Sjöberg, Y. Karayiannidis, “On the stability of admittance control for physical human-robot interaction under delays,” submitted to *IEEE Transactions on Mechatronics*.

[B] **R. Jaberzadeh Ansari**, G. Giordano, J. Sjöberg, Y. Karayiannidis, “Human grasp position estimation for human-robot cooperative object manipulation,” *Robotics and Autonomous Systems*, vol. 131, no. 103600, 2020.

[C] **R. Jaberzadeh Ansari**, Y. Karayiannidis, “Task-based role adaptation for human-robot cooperative object handling,” *IEEE Robotics and Automation Letters*, vol. 6, no. 2, pp. 3592-3598, 2021.

Other related publications of the Author not included in this thesis:

- **R. Jaberzadeh Ansari**, Y. Karayiannidis, J. Sjöberg, “Physical human-robot interaction through a jointly-held object based on kinesthetic perception,” *27th IEEE International Symposium on Robot and Human Interactive Communication (RO-MAN)*, Nanjing, China, 2018. **Awarded Nanjing City Prize in IEEE RO-MAN 2018.**
- **R. Jaberzadeh Ansari**, Y. Karayiannidis, “Reducing the human effort for human-robot cooperative object manipulation via control design,” *20th World Congress of the International Federation of Automatic Control (IFAC)*, Toulouse, France, 2017.

Acronyms

Cobot:	Collaborative Robot
CPE:	Contact Point Estimation
DMP:	Dynamic Primitive Motions
DoF:	Degrees of Freedom
F/T:	Force/Torque
GPE:	Grasp Position Estimation
HRC:	Human-Robot Collaboration
IO:	Input-Output
LSM:	Least-Squares Method
MD:	Maximum Deviation
MILP:	Mixed-Integer Linear Programming
PHRI:	Physical Human-Robot Interaction
PHRC:	Physical Human-Robot Collaboration
RLS:	Recursive Least Squares
SMEs:	Small and Medium-sized Enterprises

Contents

Abstract i

Acknowledgments iii

List of Publications v

Acronyms vii

Contents ix

I Introductory Chapters 1

1 Introduction 3

1.1 Thesis outline 5
1.2 Contributions of the author 6

2 Interaction Control under Time Delay 9

2.1 Overview 9
2.2 Problem formulation 10
2.3 Stability analysis of uncoupled and coupled system 12
Uncoupled system 12

Coupled system 13
2.4 Case study 1: Physical human–robot interaction with a passive/active human model 15
2.5 Case study 2: Direct PHRI 17

3 Human Grasp Position Estimation 19
3.1 Overview 19
3.2 Problem formulation 20
3.3 Parameter estimation algorithm 24

4 Task-based Role Adaptation in Shared Object Manipulation 29
4.1 Overview 29
4.2 Interaction dynamics of shared object manipulation 30
Robot dynamics 31
Constraints 32
Interaction dynamics 32
4.3 Role allocation 33
4.4 Task adaptation 34

5 Conclusion and Future Work 37

References 39

II Included Papers 47

A On the Stability of Admittance Control for Physical Human-Robot Interaction under Delays A1
1 Introduction A3
2 Problem description A6
2.1 Generic modeling of a 1-DoF PHRI system A7
2.2 Modeling of uncoupled and coupled system A7
2.3 Stability analysis A11
3 Time delayed system A12
3.1 Experimental results A18
4 Conclusions A26
Appendix A - Derivation of passivity and stability of sys_4 . . . . . . A26
References A28

B Human Grasp Position Estimation for Human-Robot Cooperative Object Manipulation B1

1 Introduction B3
2 Related works B5
3 Background B6
    3.1 Object dynamics B6
    3.2 Parameter estimation B8
4 Models for human grasp localization using kinesthetic information B9
    4.1 Model considering $\boldsymbol{\tau}_h$ as a disturbance input B9
    4.2 Model considering $\boldsymbol{\tau}_h$ as an unknown parameter B10
5 Proposed estimation scheme B10
    5.1 Qualifying the input data B11
    5.2 Qualifying the estimates B12
    5.3 Modified recursive least-squares algorithm B13
6 Validation of the proposed estimation scheme B14
    6.1 Experimental setup for data collection B15
    6.2 Quality of the model B16
    6.3 Accuracy of the estimation B17
7 Results B18
    7.1 Experimental results B18
8 Conclusions B26
References B27

C Task-Based Role Adaptation for Human-Robot Cooperative Object Handling C1

1 Introduction C3
2 Related works C4
3 Problem formulation C6
    3.1 Notation C6
    3.2 Rigid-body dynamics C7
    3.3 Robot and interaction dynamics C8
    3.4 Problem statement C9
4 Proposed controller C10
    4.1 Task encoding C10
    4.2 Active task identification C12
    4.3 Role allocation C13

5 Results C14
  5.1 Simulation studies C14
  5.2 Experimental studies C17
6 Conclusions and future work C18
References C23

Part I

Introductory Chapters

CHAPTER 1

Introduction

As technology advances, robotics is continuously transforming production industries and services. Traditionally, robots have been used for tedious, precise tasks, especially in the manufacturing industry. Traditional robots require a well-designed bounded workspace, which makes them unjustifiable for rapid deployment and application in Small and Medium-sized Enterprises (SMEs). This requirement also limits the use of robotic systems in non-manufacturing industries such as healthcare.

Collaborative robots (cobots) offer a flexible solution to overcome the limitations of traditional robots. The main reasons for employing cobots include higher accuracy, time and energy savings, economic benefits, and consistent help for humans. But most importantly, cobots are safe to operate in the vicinity of humans (Fig. 1.1) as new regulations apply to their hardware and software designs [1], [2]. These characteristics allow for faster deployment and result in a safer and more productive collaboration between humans and robots for the purpose of accomplishing tasks.

Cobots have a variety of potential applications, including assembly assistance [3], rescue robotics [4], space applications [5], and social care [6]. The main tasks are predicted to be pick & place, assembly, and handling of materials [7]. A current application is the use of cobots in the COVID-19 pandemic in health and non-health sectors. Undoubtedly, COVID-19 has raised standards for cleaning and hygiene. According to [8], [9], although the new cleaning requirements pose a challenge for a segment of society that relies heavily on humans and their skills, cobots have effectively mitigated this issue, especially in hospitals and common areas such as workplaces, factories, and department stores, delivering healthcare and safety to society [10].

The growing demand for cobots in various fields, e.g., production, healthcare, mining, and manufacturing, requires high levels of cooperation between robots and humans [11]. Humans must be aware of the ongoing operation of the robot, and the robot should be able to interpret a human's command correctly and deal with the intentions and movements of the human [12]. Comprehensive interpretations require that the robots receive sufficient and accurate information through communication channels with the humans. The main communication channels in Human-Robot Interaction (HRI) are vision and haptics [13]–[16], but other communication channels such as sound [17] and electromyography (EMG) signals [18], [19] are also possible.

The haptic channel is distinguished from other communication channels through the bidirectional exchange of mechanical energy between the robot and the human [20]. The information that can be obtained from this channel includes the measured interaction force, which can then be used to study Physical Human-Robot Interaction (PHRI) and to design perception and control algorithms [21]–[27].

A paramount objective in PHRI is to ensure safety. One of the safety aspects is the stability of the human-robot control system, which can be compromised by various factors such as internal time delays. Internal delays in the control loop system increase the possibility of instability and more oscillations when the human grasps the robot firmly, i.e., the stiffness of the human hand is high. There are several studies that focus on the delay and derive stability conditions on the controller parameters by approximating the delay, but in many cases the approximation of the delay does not lead to an accurate stability boundary. Another safety aspect is the mutual understanding between human and robot to avoid conflicts in the execution of a task. Interpretation of human intention is challenging when human force/torque is not directly measured. The applied human force/torque represents the human intention in case of direct measurement. However, with a distance between robot and human, such as in shared object manipulation, a mapping of human forces that does not correspond to human intention is measured. Furthermore, shared object manipulation in physical human-robot interaction may require extra effort from the human side, which is not desirable especially for repetitive tasks. If the task is known, the desired trajectory for the robot can be determined and thus the robot can actively participate in the task. However, in a generic object-handling scenario, the task is typically unknown and thus the robot's role cannot be assigned.

The thesis focuses on perception and control algorithms for physical human-robot interaction. It is devoted to investigating safety aspects, such as stability, and to addressing the challenges of identifying and responding to human haptic commands. The thesis investigates the effect of internal delay on direct PHRI. A generic mathematical formulation for modeling the PHRI system is developed and compared with similar studies on stability in PHRI. An analysis approach is also proposed to analytically derive the stability conditions for the design parameters. The thesis also investigates the shared human-robot object manipulation. An estimation algorithm based on the Recursive Least-Squares (RLS) method is developed to estimate the human grasp position. The estimation algorithm is tested and validated with simulation and experimental data. Finally, the thesis introduces a control scheme for shared object manipulation. We assume that the human determines the target position of the object and that the cobot assists the human by applying a percentage of the force required to move the object. In order to reduce the human effort, the ongoing task is compared with the known tasks, which are defined as dynamical systems, and in case of a similar velocity profile, the robot assists with the identified task based on a predefined load share. In particular, primitive motions are encoded as separate tasks; this allows human effort in generic object manipulation to be reduced.

1.1 Thesis outline

The thesis consists of two main parts. Part I is a summary of the research area, concepts, and proposed methods. In this regard, Chapter 2 focuses on the modeling of time-delay in physical human-robot interaction and presents the proposed approach to analyze the stability of such systems. Chapter 3 introduces the human grasp position estimation problem and the proposed

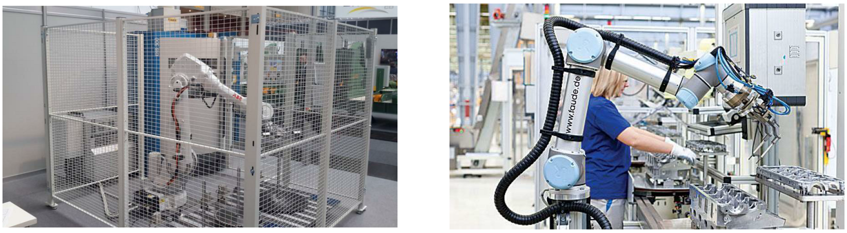

Figure 1.1: Non-collaborative robots vs collaborative robots (cobots) [28].

estimation scheme. Chapter 4 presents the interaction dynamics from which the control scheme for shared human-robot object manipulation is derived and the role of the robot is formulated. In addition, task definition and identification and the assignment of the robot's role based on the identified task are discussed. Chapter 5 summarizes the appended papers, offers concluding remarks, and comments on future work. The papers appended to this thesis are given in Part II.

1.2 Contributions of the author

Paper A: On the stability of admittance control for physical human-robot interaction under delays
Summary of contributions: In this paper, we address the effect of time delay on the stability of a time-delayed PHRI system and derive the stability conditions analytically. Using the derived conditions, we evaluate the effect of backdrivability and first-order filtering on the stability of the system. Finally, we show how the derived conditions can be used to experimentally evaluate a PHRI system.
Individual contribution: The author proposed the analysis method, planned, implemented, and processed the simulations and experiments, and took the main responsibility in writing the paper as the lead author.

Paper B: Human grasp position estimation for human-robot cooperative object manipulation
Summary of contributions: This paper addresses the estimation of human grasp position in an object-handling scenario in PHRI. Knowing the human

grasp position is a key factor enabling the human to manipulate an object smoothly when this object is also handled by the robot. To achieve this, we proposed a new estimation algorithm that modifies the recursive least squares method. The proposed estimation method is developed to estimate the position of the human grasp even when the human applies force and torque simultaneously. We evaluated the proposed method through simulation and experimental studies.
Individual contribution: The author developed the estimation method, implemented the algorithm, planned, implemented, and processed the simulations and experiments, and took the main responsibility in writing the paper as the lead author.

Paper C: Task-based role adaptation for human-robot cooperative object handling
Summary of contributions: This paper focuses on the shared human-robot object handling. We proposed a new control scheme to reduce the human effort without restricting the degrees of freedom. The proposed method includes three main parts: controller, task encoding, and role allocation. The controller is designed to have stable closed-loop interaction dynamics. The task coding is performed using the dynamical system. Moreover, the primitive motions are defined as separate tasks. Finally, using the interaction dynamics, the desired force for each task is used to increase the role of the robot and reduce the human effort. The proposed method is validated by simulation and experimental studies.
Individual contribution: The author proposed the control algorithm, planned, implemented, and processed the simulation and experimental studies, and took the main responsibility in writing the paper as the lead author.

CHAPTER 2

Interaction Control under Time Delay

In PHRI, system stability is important to human safety. This chapter gives an overview of the stability problem in the presence of a time delay in a direct PHRI. We start by formulating the problem and deriving the closed-loop dynamics of the system. We then describe an approach to evaluating the stability of the system by analyzing the location of its pole. We also review the proposed approach for determining the stability conditions and discuss two study cases in detail.

2.1 Overview

The PHRI system consists of an uncoupled system (robot and force sensor) and a human, shown in Fig. 2.1. The stability of the coupled system (the uncoupled system and human) is affected by 1) system parameters, e.g., time delay [29], [30], human hand stiffness [31], sampling time [32], and the robot's inertia and damping [32], and 2) design parameters used in the controllers and filters [31]. Multiple approaches for studying the stability of PHRI systems have been proposed, including passivity-based methods [29], [30], [32]–[34], pole placement [35], Lyapunov theory [31], [36], and online monitoring of high frequency oscillations of the force signal [37], [38].

This thesis investigates the effect of a time delay on the stability of the system. The delay is introduced either by the components of the system, such as the admittance controller and force filter, or by the communication channel and computation steps. The evaluation of stability by approximating the time delay [31], [36] using Taylor series expansion or Pade approximation [39] may lead to inaccurate stability conditions [36], and employing the passivity-based methods may result in conservative stability conditions [37], [40]. This thesis models the time delay with exponential functions and proposes a new approach to calculating the stability conditions analytically.

This chapter discusses a direct physical human-robot collaboration scenario with a non-backdrivable robotic manipulator and a time delay, either in the force sensor or in the internal control of the robot, and presents an analytical approach to evaluating the stability of such a system.

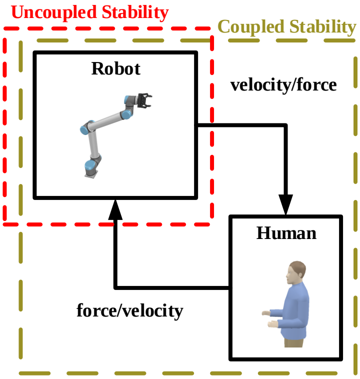

Figure 2.1: A typical physical human-robot interaction.

2.2 Problem formulation

The block diagram of a setup for direct physical human-robot interaction is shown in Fig. 2.2. The uncoupled system is the closed-loop dynamics of the robotic system and is described in the Laplace domain by the transfer function G_{us}. Robotic systems in PHRI can be categorized as impedance or admittance based on the causal relationship between force and velocity [41]. Robots of

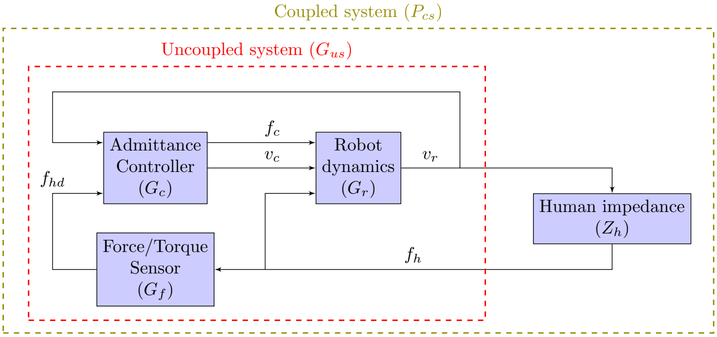
Coupled system (P_{cs})
Uncoupled system (G_{us})
Admittance Controller (G_c)
Robot dynamics (G_r)
Human impedance (Z_h)
Force/Torque Sensor (G_f)
f_c
v_c
v_r
f_{hd}
f_h

Figure 2.2: Block diagram of a PHRI system.

the impedance type generate forces based on the motion deviation and are typically backdrivable and lightweight. Robots of the admittance type deviate from the desired motion based on the interaction force and are typically non-backdrivable, such as commercial industrial robots. In this thesis, we consider the uncoupled system as an admittance robotic system; this means that the input is the measured interaction force and the output of the robotic system is the velocity. The robotic system and the human constitute the coupled system, which is described by the closed-loop dynamics for the robot velocity v_r; i.e., $P_{cs}v_r = 0$, where P_{cs} is a function in the Laplace domain. The following components constitute the dynamics of the coupled system:

- **Robot dynamics (G_r):** The mathematical model of the robotic manipulator is given by

$$v_r = \begin{bmatrix} G_{r1} & G_{r2} & G_{r3} \end{bmatrix} \begin{bmatrix} f_c \\ v_c \\ f_h \end{bmatrix} \tag{2.1}$$

  where $f_h \in \mathbb{R}$ is the applied force by the human, and $f_c, v_c \in \mathbb{R}$ stand for the force command and velocity command, respectively. The transfer functions G_{r1}, G_{r2}, and G_{r3} describe a force control robot, a velocity-control robot, and a backdrivable/non-backdrivable robot, respectively.

- **Interaction Controller (G_c):** The reference force and velocity for the robot are generated by the controller formulated as:

$$\begin{bmatrix} f_c \\ v_c \end{bmatrix} = \begin{bmatrix} G_{c11} & G_{c12} \\ G_{c21} & G_{c22} \end{bmatrix} \begin{bmatrix} v_r \\ f_{hd} \end{bmatrix} \tag{2.2}$$

where $\boldsymbol{G}_c$ describes the admittance, impedance, or mixed impedance-admittance controller. The pure impedance-type controller generates force using the input velocity, i.e., $G_{c11} \neq 0$, and the pure admittance-type controller generates velocity using the measured force, i.e., $G_{c22} \neq 0$.

- **Force sensor (G_f):** The force applied by the human is measured by a Force/Torque (F/T) sensor installed at the robot's end-effector, which is described by G_f.
- **Human dynamics (Z_h):** The human dynamics are described by Z_h. The human can be considered as a passive linear system [32], an impedance with mass, damping, and stiffness [31], [42], or a combination of passive/active elements [35], [36].

2.3 Stability analysis of uncoupled and coupled system

In this thesis, we evaluate the passivity of the individual parts, and the stability of the closed-loop system.

Uncoupled system

The uncoupled system includes the F/T sensor, the admittance controller, and the robot dynamics. The input to the uncoupled system is the applied force of the human f_h, and the output is the velocity of the end-effector of the robot v_r. The transfer function of the uncoupled system G_{us}, shown in Fig. 2.2, is derived as follows:

$$G_{us} = \frac{G_f G_{c12} G_{r1} + G_f G_{c22} G_{r2} - G_{r3}}{G_{c11} G_{r1} + G_{c21} G_{r2} - 1} \tag{2.3}$$

Assuming that the human is passive, the passivity of the uncoupled system results in the stability of the coupled system. A linear time-invariant system described with the transfer function model $v_r = G_{us} f_h$ is passive if and only if the transfer function G_{us} is positive real [39]. Before stating the definition of positive realness, we need to review the definition of a rational transfer function and analytic transfer function:

Definition 1: *A transfer function is said to be rational if it can be written in the form*

$$H(s) = K\frac{P(s)}{Q(s)} \tag{2.4}$$

where the scalar K is called the gain, $P(s)$ is a polynomial in the complex variable s of degree m, and $Q(s)$ is a polynomial of degree n [39].

Definition 2: *An irrational transfer function is said to be analytic in a region if it is defined and continuous in that region [39].*

The positive real of a transfer function can be defined as follows [39], [43]:

Definition 3: *The rational or irrational function $G_{us}(s)$ is positive real if*

- *$G_{us}(s)$ is analytic for all $Re[s] > 0$.*
- *$G_{us}(s)$ is real for all positive and real s.*
- *$Re[G_{us}(s)] \geq 0$ for all $Re[s] > 0$.*

Coupled system

The closed-loop dynamics of the coupled system includes the uncoupled dynamics and the human dynamics. By considering the velocity of the robot v_r as the state of the system, the characteristic equation of the coupled dynamics is given by:

$$\begin{aligned} P_{cs} v_r \coloneqq (&G_{c11}G_{r1} + G_{c21}G_{r2} + G_{r3}Z_h \\ &-G_f G_{c12} G_{r1} Z_h - G_f G_{c22} Z_h G_{r2} - 1)\, v_r = 0 \end{aligned} \tag{2.5}$$

For a time-delayed system with a single delay, the characteristic equation (2.5) has the form $P_h(s,T) \equiv A(s) + B(s)e^{-sT}$, where $A(s)$ and $B(s)$ are polynomials of degrees n_A and n_B, respectively. The systems with $n_A > n_B$, $n_A = n_B$, and $n_A < n_B$ are referred as retarded, neutral, and advanced, respectively. In this thesis, only the retarded characteristic equations are considered. Also, we assume that $A(s)$ and $B(s)$ do not have common imaginary roots and that $A(0) + B(0) \neq 0$. Otherwise, the $P_h(s,T)$ is unstable for all $T \geq 0$.

To derive stability conditions, we use the direct method where the system poles, i.e., the roots of the characteristic equation (2.5), are evaluated. The system is stable if all the poles are in the left half-plane (LHP). Assuming that $A(s)$ and $B(s)$ have no common imaginary roots and that $A(0) + B(0) \neq 0$, the direct method is employed to check the location of poles [44]. The number of roots is infinite for $P_h(s,T)$ when $T \neq 0$ because of the complex exponential function e^{-sT} [45], [46]. However, roots of $P_h(s,T)$ change continuously with respect to T. This means that as T changes, the roots may cross the imaginary axis from the LHP to the RHP (i.e., become unstable) and vice versa (i.e., become stable). Thus, to evaluate the roots of the characteristic equation, first, the roots of $P_h(s,T)$ for $T = 0$ are evaluated. Since $P_h(s,0)$ is a polynomial, the number of roots is finite. If $P_h(s,0)$ has roots in RHP then the system is unstable for all values of T. Otherwise, the imaginary crossing of the roots must be checked for $T \neq 0$. Expanding $P_h(s,T) = 0$ for $s = \pm\omega j$ yields [45], [46]:

$$\begin{cases} A(\omega j) + B(\omega j)e^{-\omega T j} = 0 \\ A(-\omega j) + B(-\omega j)e^{\omega T j} = 0 \end{cases} \tag{2.6}$$

Eliminating the exponential terms results in the delay-independent equation

$$A(\omega j)A(-\omega j) - B(\omega j)B(-\omega j) = 0 \tag{2.7}$$

which is a polynomial equation in ω^2. The potential imaginary crossings of the roots are given by the non-negative roots of (2.7). For the positive roots, the time delays satisfying $P_h(s,T) = 0$ can be derived using the phase equation of $P_h(s,T) = 0$ as follows:

$$\omega_c T_0 = \arg\left\{-\frac{B(\omega_c j)}{A(\omega_c j)}\right\} + 2\pi k, \qquad k = 0, 1, ... \tag{2.8}$$

where ω_c is the root of (2.7). If the delay T is less than T_0, the roots do not cross the imaginary axis and thus the system is stable.

In summary, to check the stability of the time-delayed system with the retarded characteristic equation, the stability for the non-delayed system, i.e., $P_h(s,0)$, is first determined. If the system is stable, ω_c is calculated by finding the roots of (2.7). In the case of negative or complex ω_c, the system is stable for all time delays. In the case of positive real ω_c, T_0 is computed; and the system is stable for time delays $T < T_0$.

2.4 Case study 1: Physical human–robot interaction with a passive/active human model

The first case study uses the 1-DoF PHRI system described in [36]. In [36], the robot is modeled by an integrator, while the human model consists of a passive and an active part. The passive part is modeled as a mechanical mass-damper-spring system that corresponds to the dynamical model of the human arm. The active part of the human dynamics is modeled as a PD-controller with proportional and derivative gains that react to the velocity of the system. The mathematical model of this setup is given by:

$$\begin{cases} G_r(s) = \begin{bmatrix} 0 & 1 & 0 \end{bmatrix} \\ G_c(s) = \dfrac{1}{m_c s + c_c} \begin{bmatrix} 0 & 0 \\ -\frac{k_e}{s} & 1 \end{bmatrix} \\ G_f(s) = 1 \\ Z_h(s) = -(m_h s + c_h + \dfrac{k_h k_e}{s} + e^{-Ts}(k_d + \dfrac{k_p k_e}{s})) \end{cases} \tag{2.9}$$

where $m_c, c_c \in \mathbb{R}$ are the admittance controller parameters, $k_e \in \mathbb{R}$ is the stiffness of the virtual environment, $m_h, c_h, k_h \in \mathbb{R}$ are the human's arm mass, damping, and stiffness, respectively, and $k_p, k_d \in \mathbb{R}$ denote derivation and proportional gains of the active part of the human model, respectively. Finally, $T \in \mathbb{R}$ denotes time-delay in the human's response time.

Müller *et al.* proposed sufficient stability conditions, based on the Lyapunov-Krasovskii functional [47], for the stability analysis of a stationary point for a special type of nonlinear time-delay systems, and they employed it to analyze the aforementioned PHRI system. The stability conditions for (2.9) proposed by Müller *et al.* [36] are given by:

$$\begin{cases} (c_c + c_h) - |k_d| > T|k_p| \\ k_e(1 + k_h) + k_p > 0 \end{cases} \tag{2.10}$$

They compare these stability conditions with those derived using Colgate's passivity condition [32], and the Routh-Hurwitz stability condition for systems with time-delay approximations, which are first-order Taylor expansion series, and first-order Pade-approximation [39], as shown in Fig. 2.3. They conclude that their proposed stability conditions are more accurate than the conditions derived by time-approximation, and also less conservative than Colgate's passivity condition.

To evaluate our approach, the stability criterion using the direct method is calculated. To this aim, first the characteristic equation of system (2.9) is derived using (2.5) and given by:

$$P_h(s,T) = (m_c + m_h)s^2 + (d_c + d_h)s + k_e + k_h k_e + (k_d s + k_p k_e)e^{-Ts} \quad (2.11)$$

Then, the stability region is derived using the direct method and presented in Fig. 2.3. Using the direct method, the poles of the characteristic equation are examined. Since we consider the delay as an exponential term, the derived stability region is accurate. The stability regions found by the proposed condition (2.10) and Colgate's passivity condition are conservative, and the ones found by time-approximation methods are not accurate and give false stability regions.

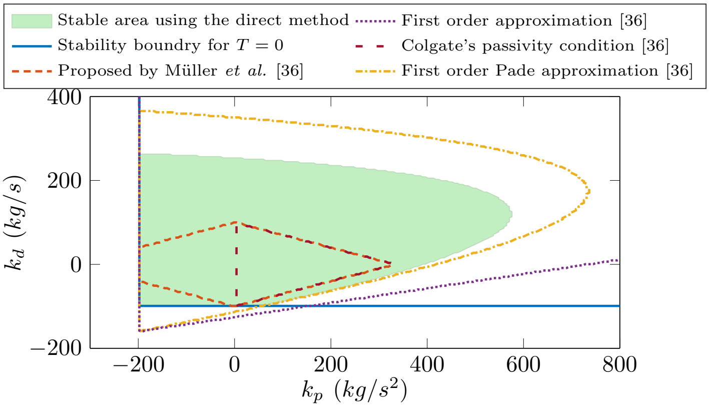

Figure 2.3: Comparison of stability region for parameters k_p and k_d calculated using the direct method with the stability regions calculated using stability conditions of [36].

2.5 Case study 2: Direct PHRI

A typical setup of direct interaction between a human and a robot is shown in Fig. 2.4. The setup includes a UR10 collaborative robot, an OptoForce F/T sensor, and a light handle to interact with the robot. Also, a laser pointer is installed on the handle. The robot is velocity-controlled and is modeled by a first-order filter following the velocity input with delay T. The F/T sensor is modeled with a first order filter. In this thesis, we consider a linear impedance to model the human arm. Details on such models are given in [48]. The mathematical model of such a setup for 1-DoF is given by:

$$\begin{cases} G_r(s) = e^{-Ts}\begin{bmatrix} 0 & \frac{1}{m_r s + c_r} & 0 \end{bmatrix} \\ G_c(s) = \begin{bmatrix} 0 & 0 \\ 0 & \frac{1}{m_c s + c_c} \end{bmatrix} \\ G_f(s) = \dfrac{1}{T_f s + 1} \\ Z_h(s) = -(m_h s + c_h + \dfrac{k_h}{s}) \end{cases} \tag{2.12}$$

where $m_r, c_r \in \mathbb{R}$ are the apparent inertia and damping of the robotic manipulator, respectively. $T \in \mathbb{R}$ is the internal delay in the communication channel of the reference velocity; $m_c, c_c \in \mathbb{R}$ are the admittance controller parameters; and $T_f \in \mathbb{R}$ is the time constant of the force filter.

In paper A, the mathematical model (2.12) is first compared to studies with similar PHRI setups, such as [31], [35], [36]. The comparisons are made across three topics: the method of stability analysis, backdrivability of the robot manipulator, and modeling of delay. The majority of the studies evaluate the stability of the coupled system with the delay. Also, backdrivable manipulators have been studied more than the non-backdrivable robots for time-delayed PHRI systems. Then, the effect of first-order filtering and backdrivability on the stability of the coupled system of (2.12) is evaluated separately. We show that although a backdrivable robot is a passive robotic system, converting a non-backdrivable robot to a backdrivable robot does not result in a passive robotic system in the presence of a delay in command or force data. Finally, we conducted an experimental study in which an operator grasps the handle on the end effector of the robot and attempts to stabilize the laser spot on the given target. We show how the proposed approach can be used to analyze the stability of the interaction. The reader is referred to Paper A for more

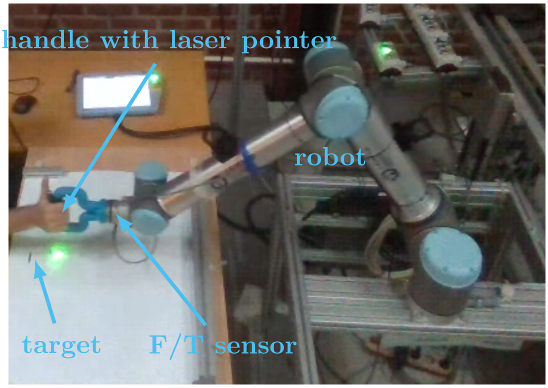
handle with laser pointer
robot
target
F/T sensor

Figure 2.4: Physical Human-Robot Interaction setup. The operator grabs the handle to turn on the laser and then moves the laser to the target point.

details.

CHAPTER 3

Human Grasp Position Estimation

This chapter addresses the problem of estimating the human grasp position in physical human-robot interaction. The chapter also reviews the challenges involved and possible strategies to overcome them.

3.1 Overview

Shared object handling is a common task in PHRI, see Fig. 3.1 for an example. In such scenarios, the robot typically measures the interaction force at its end effector. When a human applies the force there, at the end effector, the measurement represents the human's intention and the direction of motion [21], [26], [27]. However, when the interaction involves a jointly held object, the human applies force at a grasp position that is at a distance from the force sensor. In this case, the measurement of the force applied by the human may not represent the human's intent [22], [25], [49]. To overcome this problem, we showed that the intention of the human can be interpreted correctly if the grasp position is known [50]. By knowing the human grasp position, the force applied by the human can be calculated from the measured force at the end-effector of the robot, and the command for the robot can be calculated based on the calculated human force. If no torque is exerted at the grasp position of the human, the estimation of the human grasp position is simplified to contact point estimation, which is a well-studied topic in robotics [51]–[58]. In this regard, the contact point can be estimated by approaches such as the least squares method [59], particle filters [53], and machine learning [56], [58]. The contact point is estimated for various purposes such as calibration of a tool by simultaneously estimating the tool-tip and the normal direction of the contact surface [52], and keeping an object horizontal with robot assistance [60]. In contact point estimation, the measured force and torque are sufficient for estimation of the contact point [55]. However, estimating the human grasp position is challenging in the case of a "grasp" that involves simultaneous torques and forces. The measured force and torque data may not be enough for the estimation of the human grasp position, and additional data such as the velocity and acceleration of the human hand may be required [59]. We extend contact point estimation algorithms to enable human grasp position estimation in this more challenging case. Unlike [59], our method does not require any additional data beyond the force and torque measured at the robot's end-effector. This chapter also presents the derivation of the proposed estimator.

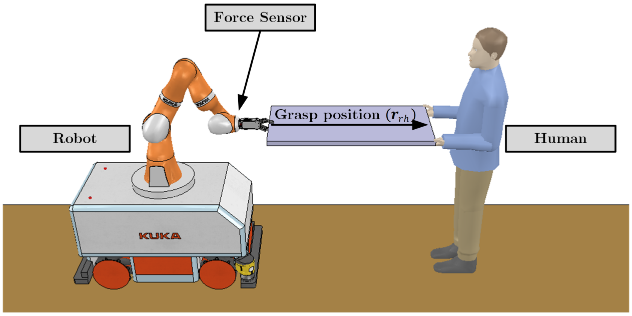

Figure 3.1: Shared object-handling scenario.

3.2 Problem formulation

The free-body diagram of an object interacting with a robot and a human is shown in Fig. 3.2. The position and orientation of a rigid object is described

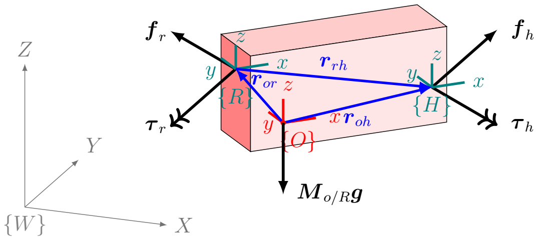

Figure 3.2: Free-body diagram of an object.

using six independent parameters denoted by $\boldsymbol{x}_o = [\boldsymbol{p}_o^T, \boldsymbol{\phi}_o^T]^T \in \mathbb{R}^6$, where the vector $\boldsymbol{p}_o \in \mathbb{R}^3$ represents the position of the object's center of mass and the vector $\boldsymbol{\phi}_o \in \mathbb{R}^3$ denotes the orientation of the fixed body frame located at the center of mass. The vector $\boldsymbol{v}_o = [\dot{\boldsymbol{p}}_o^T, \boldsymbol{\omega}_o^T]^T \in \mathbb{R}^6$ represents linear and angular velocities, where $\boldsymbol{\omega}_o = \boldsymbol{T}(\boldsymbol{\phi}_o)\dot{\boldsymbol{\phi}}_o$ and $\boldsymbol{T}(\boldsymbol{\phi}_o)$ depends on the sequence of the Euler angles. The dynamics of an object with six degrees of freedom with respect to its center of mass are given by [61]:

$$\boldsymbol{M}_o(\boldsymbol{x}_o)\dot{\boldsymbol{v}}_o + \boldsymbol{C}_o(\boldsymbol{x}_o, \boldsymbol{v}_o) + \boldsymbol{g}_o(\boldsymbol{x}_o) = \boldsymbol{h}_o \tag{3.1}$$

where:

- $\boldsymbol{M}_o(\boldsymbol{x}_o) \in \mathbb{R}^{6\times 6}$ is the object inertia matrix:

  $$\boldsymbol{M}_o(\boldsymbol{x}_o) = \begin{bmatrix} m\boldsymbol{I}_{3\times 3} & \boldsymbol{0}_{3\times 3} \\ \boldsymbol{0}_{3\times 3} & \boldsymbol{J}_o(\boldsymbol{x}_o) \end{bmatrix} \tag{3.2}$$

  where $\boldsymbol{J}_o(\boldsymbol{x}_o) \in \mathbb{R}^{3\times 3}$ is the moment of inertia relative to the center of mass of the object, and expressed in the world frame $\{W\}$,

- $\boldsymbol{C}_o(\boldsymbol{x}_o, \boldsymbol{v}_o) \in \mathbb{R}^6$ is the Coriolis vector:

  $$\boldsymbol{C}_o(\boldsymbol{x}_o, \boldsymbol{v}_o) = \begin{bmatrix} \boldsymbol{0}_{3\times 1} \\ [\boldsymbol{\omega}_o]_\times \boldsymbol{J}_o \boldsymbol{\omega}_o \end{bmatrix} \tag{3.3}$$

  where $[\boldsymbol{\omega}_o]_\times \in \mathbb{R}^{3\times 3}$ is the skew-symmetric matrix employed to replace a cross product with a matrix product,

- $\boldsymbol{g}_o(\boldsymbol{x}_o) \in \mathbb{R}^6$ is the gravity vector:

  $$\boldsymbol{g}_o(\boldsymbol{x}_o) = -\boldsymbol{M}_o\boldsymbol{g} \tag{3.4}$$

  where $\boldsymbol{g} \in \mathbb{R}^6$ is the gravity vector defined with respect to the world frame,

- $\boldsymbol{h}_o \in \mathbb{R}^6$ is the total external wrench, i.e., force and torque, applied on the object:

  $$\boldsymbol{h}_o = \begin{bmatrix} \boldsymbol{f}_o \\ \boldsymbol{\tau}_o \end{bmatrix}. \tag{3.5}$$

  where $\boldsymbol{f}_o \in \mathbb{R}^3$ and $\boldsymbol{\tau}_o \in \mathbb{R}^3$ are the total external force and torque applied on the object, respectively.

Considering n_A contact points of the object with the environment and grasp positions with agents, i.e., human and robot, the external wrench applied on the object is given by:

$$\boldsymbol{h}_o = \sum_{i=1}^{n_A} \boldsymbol{G}_{oi}\boldsymbol{h}_i \tag{3.6}$$

where $\boldsymbol{G}_{oi} \in \mathbb{R}^{6\times 6}$ is the grasp matrix, defined as:

$$\boldsymbol{G}_{oi} = \begin{bmatrix} \boldsymbol{I}_{3\times 3} & \boldsymbol{0}_{3\times 3} \\ [\boldsymbol{r}_{oi}]_\times & \boldsymbol{I}_{3\times 3} \end{bmatrix} \tag{3.7}$$

where $\boldsymbol{r}_{oi} \in \mathbb{R}^3$ presents the position of contact or grasp point i and $[\boldsymbol{r}_{oi}]_\times \in \mathbb{R}^{3\times 3}$ is the skew-symmetric matrix employed to replace a cross product with a matrix product. Finally, $\boldsymbol{h}_i \in \mathbb{R}^6$ is the external wrench applied by the agent i on the object:

$$\boldsymbol{h}_i = \begin{bmatrix} \boldsymbol{f}_i \\ \boldsymbol{\tau}_i \end{bmatrix} \tag{3.8}$$

where $\boldsymbol{f}_i \in \mathbb{R}^3$ and $\boldsymbol{\tau}_i \in \mathbb{R}^3$ are the external force and torque applied by the agent i, respectively. In the contact-point case, $\boldsymbol{\tau}_i$ is assumed to be zero.

Since all the measurements are available for the robot end-effector frame $\{R\}$, it is more convenient to derive the object dynamics with respect to this frame. The object dynamics can be written as:

$$\boldsymbol{M}_{o/R}\dot{\boldsymbol{v}}_{o/R} + \boldsymbol{C}_{o/R} + \boldsymbol{g}_{o/R} = \boldsymbol{h}_r + \boldsymbol{G}_{rh}\boldsymbol{h}_h \tag{3.9}$$

where

- $\boldsymbol{x}_{o/R}$ denotes the position and the orientation of the object, measured at the origin of the frame $\{R\}$ and $\boldsymbol{v}_{o/R}$ the translational and angular velocities of the object, measured at the origin of the frame $\{R\}$,
- $\boldsymbol{M}_{o/R}$ is the object inertia matrix defined with respect to the origin of the frame $\{R\}$:
  $$\boldsymbol{M}_{o/R} = \begin{bmatrix} m\boldsymbol{I}_{3\times3} & m[\boldsymbol{r}_{or}]_\times \\ -m[\boldsymbol{r}_{or}]_\times & \boldsymbol{J}_{o/R} \end{bmatrix} \tag{3.10}$$
  where $\boldsymbol{J}_{o/R} = \boldsymbol{J}_o - m\boldsymbol{I}_{3\times3}[r_{ro}]_\times[r_{ro}]_\times$,
- $\boldsymbol{C}_{o/R}$ is the Coriolis vector defined with respect to the origin of the frame $\{R\}$:
  $$\boldsymbol{C}_{o/R} = \begin{bmatrix} -m\boldsymbol{\omega}_o \times (\boldsymbol{\omega}_o \times \boldsymbol{r}_{or}) \\ \boldsymbol{\omega}_o \times (\boldsymbol{J}_{o/R}\boldsymbol{\omega}_o) \end{bmatrix} \tag{3.11}$$
- $\boldsymbol{g}_{o/R}$ is the gravity vector defined with respect to the origin of the frame $\{R\}$:
  $$\boldsymbol{g}_{o/R} = -\boldsymbol{M}_{o/R}\boldsymbol{g}. \tag{3.12}$$

The unknown variables in the equation of motion (3.9) are the grasp position of the human, i.e., $\boldsymbol{r}_{rh}$ included in the term $\boldsymbol{G}_{rh}$, and the exerted wrench by the human, i.e., $\boldsymbol{h}_h$. The human force $\boldsymbol{f}_h$ can be calculated from the translational part of (3.9) and is given by the difference between the inertial forces and the forces measured by the sensor, $\boldsymbol{f}_r$, i.e.:

$$\boldsymbol{f}_h = \begin{bmatrix} m\boldsymbol{I}_{3\times3} & m[\boldsymbol{r}_{or}]_\times \end{bmatrix} (\dot{\boldsymbol{v}}_{o/R} - \boldsymbol{g}) - m\boldsymbol{\omega}_o \times (\boldsymbol{\omega}_o \times \boldsymbol{r}_{or}) - \boldsymbol{f}_r. \tag{3.13}$$

Thus, we derive a parameter vector that consists of $\boldsymbol{r}_{rh}$ and $\boldsymbol{\tau}_h$:

$$\boldsymbol{\theta} \overset{\text{def}}{=} \begin{bmatrix} {}^{R}\boldsymbol{r}_{rh} \\ \boldsymbol{\tau}_h \end{bmatrix}$$

where ${}^{R}\boldsymbol{r}_{rh}$ is the human grasp position defined with respect to frame $\{R\}$. To identify the unknown parameter $\boldsymbol{\theta}$, the rotational part of (3.9) is written in a linear regression form as follows:

$$\boldsymbol{y} = \boldsymbol{\Phi}\boldsymbol{\theta} \tag{3.14}$$

where the known output signal $\boldsymbol{y} \in \mathbb{R}^3$ is defined as:

$$\boldsymbol{y} \overset{\text{def}}{=} \boldsymbol{\tau}_r - \begin{bmatrix} -m[\boldsymbol{r}_{or}]_\times & \boldsymbol{J}_{o/R} \end{bmatrix} (\dot{\boldsymbol{v}}_{o/R} - \boldsymbol{g}) - \boldsymbol{\omega}_o \times (\boldsymbol{J}_{o/R}\boldsymbol{\omega}_o) \tag{3.15}$$

and the known input signal $\boldsymbol{\Phi} \in \mathbb{R}^{3\times 6}$ is defined as:

$$\boldsymbol{\Phi} \overset{\text{def}}{=} \begin{bmatrix} [\boldsymbol{f}_h]_\times \boldsymbol{R}_R^W & \boldsymbol{I}_{3\times 3} \end{bmatrix} \tag{3.16}$$

where $\boldsymbol{R}_R^W$ is the rotation matrix of $\{R\}$ with respect to the world frame $\{W\}$. The identification model (3.14), combined with (3.15) and (3.16), is different from typical ones used for contact point estimation in the sense that, here, the human torque, $\boldsymbol{\tau}_h$, is considered as an unknown parameter. We assume that the dynamic parameters of the object are known. However, these parameters can be identified using the method as described in [62].

3.3 Parameter estimation algorithm

The most common method for obtaining values of unknown parameters involved in dynamics is the least-squares method. This approach is used to estimate the unknown parameters for a linear model by minimizing the squares of the error between the measured/known output of the system and the computed output of the model. The general form of the least-squares method is:

$$\hat{\boldsymbol{\theta}} = \underset{\boldsymbol{\theta}}{\operatorname{argmin}} \quad \sum_{i=1}^{N} \frac{1}{2}\gamma^{N-i} \left(\|\boldsymbol{y}_i - \boldsymbol{\Phi}_i\boldsymbol{\theta}\|^2_{\boldsymbol{N}_i} + \|\boldsymbol{\theta} - \boldsymbol{\theta}_r\|^2_{\boldsymbol{W}} \right) \tag{3.17}$$

where N is the number of data points, $0 < \gamma \leq 1$ is the forgetting factor, $\boldsymbol{N}_i \in \mathbb{R}^{3\times 3}$ is the normalization gain matrix, $\boldsymbol{\theta}_r \in \mathbb{R}^6$ is the leakage value, and $\boldsymbol{W} \in \mathbb{R}^{6\times 6}$ is the leakage gain.

The least-squares problem (3.17) is solved by finding the roots of the gradient of its cost function, i.e.:

$$\nabla_{\boldsymbol{\theta}} \left(\sum_{i=1}^{N} \frac{1}{2} \gamma^{N-i} \left(\|\boldsymbol{y}_i - \boldsymbol{\Phi}_i \boldsymbol{\theta}\|^2_{\boldsymbol{N}_i} + \|\boldsymbol{\theta} - \boldsymbol{\theta}_r\|^2_{\boldsymbol{W}} \right) \right) = 0 \tag{3.18}$$

and is given by:

$$\hat{\boldsymbol{\theta}}_N = \boldsymbol{P}_N \left[\sum_{i=1}^{N} \gamma^{N-i} \left(\boldsymbol{\phi}_i^T \boldsymbol{N}_i \boldsymbol{y}_i + \boldsymbol{W} \boldsymbol{\theta}_r \right) \right] \tag{3.19}$$

where $\boldsymbol{P}_N = \left[\sum_{i=1}^{N} \gamma^{N-i} \left(\boldsymbol{\Phi}_i^T \boldsymbol{N}_i \boldsymbol{\Phi}_i + \boldsymbol{W} \right) \right]^{-1}$. For a faster estimation for online use, the solution can be written in recursive form:

$$\hat{\boldsymbol{\theta}}_N = \hat{\boldsymbol{\theta}}_{N-1} + \boldsymbol{P}_N \left(\boldsymbol{\Phi}_N^T \boldsymbol{N}_N \left(\boldsymbol{y}_N - \boldsymbol{\Phi}_N \hat{\boldsymbol{\theta}}_{N-1} \right) + \boldsymbol{W} \left(\boldsymbol{\theta}_r - \hat{\boldsymbol{\theta}}_{N-1} \right) \right) \tag{3.20}$$

and

$$\boldsymbol{P}_N = \frac{1}{\gamma} \left[\boldsymbol{P}_{N-1} - \boldsymbol{P}_{N-1} \left(\boldsymbol{P}_{N-1} + \gamma \left(\boldsymbol{\Phi}_N^T {\boldsymbol{N}_N}^{-1} \boldsymbol{\Phi}_N + \boldsymbol{W} \right)^{-1} \right)^{-1} \boldsymbol{P}_{N-1} \right] \tag{3.21}$$

Here, the goal is to estimate the human grasp position $\boldsymbol{r}_{rh}$, which is a part of the unknown parameter $\boldsymbol{\theta}$. The unconstrained least-squares method can be employed to identify $\boldsymbol{\theta}$. The challenges for estimation of the unknown parameter $\boldsymbol{\theta}$ are listed below.

(a) The data may not contain enough information to make solving the estimation problem possible. The main concept related to this problem is the Persistence of Excitation [63]. If the input signal $\boldsymbol{\Phi}$, defined in (3.16), satisfies this condition, the solution of the estimator would converge to the true parameter when $N \to \infty$ [63]. However, it is challenging to satisfy this condition in real-world human-robot interaction since the excitation should be generated by the human.

(b) The human is likely to change the grasp position to have better control over the object motion. Thus, the human grasp position may suddenly change to a new value.

(c) The human may apply a torque to the object, especially if the object is grasped with two hands. Since no assumption can be made regarding the exerted torque, $\boldsymbol{\tau}_h$ is time-varying and unpredictable.

To address the mentioned challenges, we propose modifying the least-squares method as follows:

- **Maximum deviation from mean:** Since variations in $\boldsymbol{\tau}_h$ and ${}^{R}\boldsymbol{r}_{rh}$ result in variations in the estimates, we propose to check the constancy of the estimates using the Maximum Deviation (MD) from the mean value, i.e.:

  $$\mathrm{MD}(\boldsymbol{\theta}_{(t-s_{MD})\rightarrow t}) \leq \boldsymbol{E}_{cMD} \tag{3.22}$$

  where $s_{MD} \in [0, t]$. $\boldsymbol{E}_{cMD} \in \mathbb{R}^6$ is an upper bound which is empirically chosen.

- **Force magnitude:** For small force values, the estimation problem would result in inaccurate parameter estimates. Thus, we disregard the data with small force values.

The proposed human grasp position estimation algorithm is presented in Algorithm 1, and the reader is referred to Paper B for more details. In addition, an evaluation of the proposed method is done in Paper B via simulation and experimental studies. The studies show the effect of the applied torque on the estimation of the grasp position and the performance of the proposed estimation method. In summary, the estimated human grasp position is successfully updated to the true grasp position when the human-applied torque is constant over a period of time. When the human applied torque is not constant, the estimated human grasp position also does not remain constant and varies with the applied torque. However, the final estimated human grasp position does not vary with the applied torque and remains at a previously estimated value that is considered to be reliable. As described at the beginning of the chapter, the estimated position can be employed for a better identification of the human intention in shared human-robot object handling.

Algorithm 1: Grasp Position Estimation Algorithm

```
Result: ${}^{R}\hat{\boldsymbol{r}}_{rh}$
Initialize $\boldsymbol{P}_0$ , ${}^{R}\hat{\boldsymbol{r}}_{rh}$ , $\hat{\boldsymbol{\theta}}$ , $\boldsymbol{E}_{cMD}$, $\bar{\boldsymbol{f}}$, $\bar{\boldsymbol{r}}_{rh}$, $\underline{\boldsymbol{r}}_{rh}$;
while (The estimator is running) do
    if $\|\boldsymbol{f}_h\| > \bar{\boldsymbol{f}}$ then
        $\boldsymbol{P}_k = \frac{1}{\gamma}\boldsymbol{P}_{k-1} - \frac{1}{\gamma}\boldsymbol{P}_{k-1}\boldsymbol{\Phi}_k^T \left(\boldsymbol{\Phi}_k\boldsymbol{P}_{k-1}\boldsymbol{\Phi}_k^T + \gamma\right)^{-1} \boldsymbol{\Phi}_k\boldsymbol{P}_{k-1}$
        $\hat{\boldsymbol{\theta}}_k = \hat{\boldsymbol{\theta}}_{k-1} + \boldsymbol{P}_k\boldsymbol{\Phi}_k^T \left(\boldsymbol{y}_k - \Phi_k\hat{\boldsymbol{\theta}}_{k-1}\right)$
        if $\mathrm{MD}(\boldsymbol{\theta}_{(t-s_{MD})\rightarrow t}) \leq \boldsymbol{E}_{cMD}$ then
            ${}^{R}\hat{\boldsymbol{r}}_{rh} = \min(\bar{\boldsymbol{r}}_{rh}, \max(\underline{\boldsymbol{r}}_{rh}, \hat{\boldsymbol{\theta}}_{k,1:3}))$
        end
        $k \leftarrow k + 1$
    end
end
```

CHAPTER 4

Task-based Role Adaptation in Shared Object Manipulation

In a shared object-handling scenario, it is important that the human can move the object independently in all degrees of freedom with the least possible effort. This chapter discusses interaction dynamics, role allocation, and task definition and adaptation for a shared human-robot object handling.

4.1 Overview

Fig. 4.1 shows a shared human-robot object-handling scenario in which the human and the robot collaborate to transport an object. The robot has an active role if the desired trajectory is explicitly commanded in the motion control loop, or passively follows the human's commands, typically conveyed through the haptic channel [21]. The interaction force is typically measured at the robot's end-effector and provides the data to understand the desired direction of human motion [21], [64]. We should note that the term force is sometimes used for describing both force and torque. As described in the previous chapter, an object between the human and the F/T sensor leads to measuring a distorted torque instead of the true one applied by the human, which obscures the understanding of the human intention. The sensed force can still be used to design controllers for shared object manipulation by considering a constrained motion policy [23], [49]. In the previous chapter, we showed that the human grasp position can be estimated from the distorted force measurements. Knowing the human grasp position, the human interaction force can be calculated and consequently be used to compute the true force applied by the human. In addition to interpreting the human's intention, it is important to assist the human as much as possible and to reduce their effort. For this purpose, it is necessary to determine the required effort for the ongoing task and change the role of the robot accordingly. The required effort can be calculated using the interaction dynamics [14], [65]–[67], which allows the formulation of how the effort is shared by the agents, i.e., human and robot [21], [68]. However, in a generic scenario, the desired trajectory for the robot may not be defined. For generic motions, this thesis proposes to define primitive motions based on Chasles' theorem and encode them as separate tasks. The tasks are encoded as dynamical systems, where the velocity can be calculated based on the robot's position. However, other methods such as human-human collaboration models [26], Dynamic Primitive Motions (DMPs) [69], and learning from demonstration by dynamical systems [64], [70] can also be used for task encoding. The robot's motion is compared with the encoded tasks and in the case of similar velocity profiles, one task is selected as active task. Based on the active task, a supporting force is calculated as part of the force required to move the object and the corresponding velocity command is sent to the robot. Consequently, the human effort is reduced without affecting the degrees of freedom of motion or installing an additional sensor.

This chapter describes how to define a desired trajectory for the robot from a known task and how to identify the ongoing task. Using the identified task, we propose a control strategy that reduces human effort while avoiding the translation/rotation problem.

4.2 Interaction dynamics of shared object manipulation

The free-body diagram of an object for a PHRI scenario is shown in Fig. 4.2. The object dynamics for PHRI application is reviewed in Section 3.2.

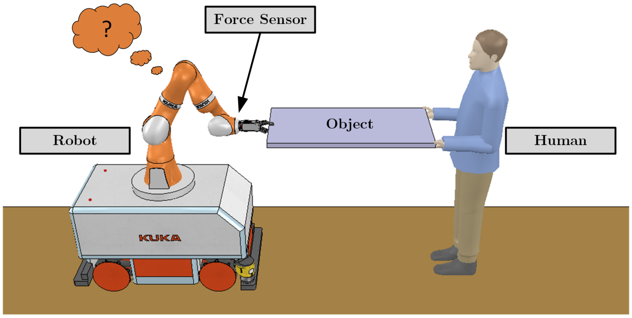
?
Force Sensor
Robot
Object
Human
KUKA

Figure 4.1: Shared object-handling scenario.

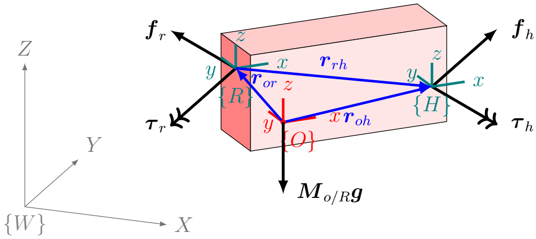
$\boldsymbol{f}_r$
$\boldsymbol{f}_h$
Z
Y
X
$\{W\}$
z
x
y
$\{R\}$
$\boldsymbol{r}_{rh}$
$\boldsymbol{r}_{or}$
z
y
x
$\{O\}$
$\boldsymbol{r}_{oh}$
z
y
x
$\{H\}$
$\boldsymbol{\tau}_r$
$\boldsymbol{\tau}_h$
$\boldsymbol{M}_{o/R}\boldsymbol{g}$

Figure 4.2: Free-body diagram of an object.

Robot dynamics

An inherently non-backdrivable collaborative robot is considered that follows the reference velocity $\boldsymbol{v}_r$ given by:

$$\boldsymbol{M}_r\dot{\boldsymbol{v}}_r = -\boldsymbol{D}_r\boldsymbol{v}_r - \boldsymbol{h}_r + \boldsymbol{u}_r \tag{4.1}$$

where $\boldsymbol{M}_r, \boldsymbol{D}_r \in \mathbb{R}^{6\times 6}$ are the diagonal matrices denoting the apparent inertia and the damping of the robotic manipulator, respectively, and $\boldsymbol{v}_i \in \mathbb{R}^6$ for $i = r, h$ are the velocities of the robot's end-effector and the human grasp point, respectively. The vector $\boldsymbol{h}_r \in \mathbb{R}^6$ denotes the force and torque applied on the robot from the object, and $\boldsymbol{u}_r \in \mathbb{R}^6$ is the control input.

Depending on the selection of the apparent inertial and damping gains of the admittance controller, different modes of control can be achieved. For example, the robot can be set to perform only translational motions by choosing sufficiently high values for the entries of $\boldsymbol{M}_r$ associated with angular acceleration, and it can be constrained to perform rotational motions about its end effector by choosing sufficiently high values for the entries of $\boldsymbol{M}_r$ associated with Cartesian acceleration.

Constraints

The human and the robot are grasping the same object, and thus they cannot move independently. In this regard, the following assumption is made:

Assumption 1. *Both the object and the connections between the object and the agents, i.e., human and robot, are assumed to be rigid.*

Due to the rigidity of the connections, both translational and rotational motions are restricted. This limitation of the movement can be formulated through kinematic constraints, defined as follows:

$$\begin{cases} \boldsymbol{x}_r = \boldsymbol{x}_h + \begin{bmatrix} \boldsymbol{r}_{hr} \\ \boldsymbol{0}_{3,1} \end{bmatrix} \\ \boldsymbol{v}_r = \boldsymbol{G}_{hr}^T \boldsymbol{v}_h \\ \dot{\boldsymbol{v}}_r = \boldsymbol{G}_{hr}^T \dot{\boldsymbol{v}}_h + \boldsymbol{c}_{v,hr} \end{cases} \tag{4.2}$$

where $\boldsymbol{x}_r, \boldsymbol{x}_h \in \mathbb{R}^6$ are position and orientation of robot's end-effector and human's grasp, respectively, $\boldsymbol{r}_{hr}$ is the vector from the human's grasp position to robot's end-effector and $\boldsymbol{c}_{v,hr}$ is given by:

$$\boldsymbol{c}_{v,hr} = \begin{bmatrix} [\boldsymbol{\omega}_o]_\times [\boldsymbol{\omega}_o]_\times \boldsymbol{r}_{hr} \\ \boldsymbol{0}_{3\times 1} \end{bmatrix} \tag{4.3}$$

Interaction dynamics

The dynamics of the object (3.9) and the robot (4.1) are coupled through the kinematic constraints (4.2). The dynamics of the coupled system with respect to the human velocity is derived by solving these equations for unknown variables $\dot{\boldsymbol{v}}_r$, $\dot{\boldsymbol{v}}_h$, and $\boldsymbol{h}_r$. The solution for $\dot{\boldsymbol{v}}_h$ is given by:

$$(\boldsymbol{M}_{o/R} + \boldsymbol{M}_r)\boldsymbol{G}_{hr}^T \dot{\boldsymbol{v}}_h = \boldsymbol{h}_{id}^{\Sigma} + \boldsymbol{G}_{rh}\boldsymbol{h}_h + \boldsymbol{u}_r \tag{4.4}$$

where

$$\boldsymbol{h}_{id}^{\Sigma} = \boldsymbol{h}_{o/R}^{\Sigma} - \boldsymbol{D}_r \boldsymbol{v}_r - (\boldsymbol{M}_{o/R} + \boldsymbol{M}_r)\boldsymbol{c}_{v,hr} \tag{4.5}$$

The system (4.4) is coupled since $\boldsymbol{M}_{o/R}$ and $\boldsymbol{G}_{rh}$ are not diagonal matrices. To decouple this system, we design $\boldsymbol{u}_r$ as follows:

$$\boldsymbol{u}_r = -\boldsymbol{h}_{id}^{\Sigma} - \boldsymbol{G}_{rh}\boldsymbol{h}_h + (\boldsymbol{M}_{o/R} + \boldsymbol{M}_r)\left(\boldsymbol{G}_{hr}^T \boldsymbol{M}_c^{-1}(\boldsymbol{h}_h + \boldsymbol{h}_t - \boldsymbol{D}_c \boldsymbol{v}_h)\right) \tag{4.6}$$

which leads to the following interaction dynamics:

$$\boldsymbol{M}_c \dot{\boldsymbol{v}}_h + \boldsymbol{D}_c \boldsymbol{v}_h = \boldsymbol{h}_h + \boldsymbol{h}_t \tag{4.7}$$

where $\boldsymbol{M}_c, \boldsymbol{D}_c \in \mathbb{R}^{6\times 6}$ are positive definite diagonal matrices and denote the apparent mass and damping of the system appearing to the human operator. The vector $\boldsymbol{h}_t$ denotes an additional control input encoding an assisting force applied on the object by the robot to help the human in a task. By employing this controller, the motion of the human directly corresponds to the applied force by the human. This means that we avoid the translation/rotation problem [22], [23], [25].

4.3 Role allocation

To move a rigid-body object along a trajectory, forces and torques must be applied. When objects are handled jointly by humans and robots, the total force required for moving the object can be applied by the human or the robot, or by both. An example is shown in Fig. 4.3, where the human and the robot are assigned to different roles for four cases that result in the same motion.

Our goal in role allocation is to reduce the human effort, when the task is known, by adjusting the role of the robot in the spectrum between active and passive. Adjusting the robot's role requires specifying a desired trajectory. For this part, we assume that the desired trajectory is given; however, we discuss how to find the desired trajectory in the next section. Given a task velocity to be tracked on the robot side with $\boldsymbol{v}_t \in \mathbb{R}^6$ and $\dot{\boldsymbol{v}}_t$, the desired force applied by the robot to adjust its role is given by:

$$\boldsymbol{h}_{ti} = \boldsymbol{C}_t \left(\boldsymbol{M}_c(\boldsymbol{G}_{rh}^T \dot{\boldsymbol{v}}_{ti} + \boldsymbol{c}_{v_{ti},rh}) + \boldsymbol{D}_c \boldsymbol{G}_{rh}^T \boldsymbol{v}_{ti}\right) \tag{4.8}$$

where $\boldsymbol{C}_t = \mathrm{diag}(c_{ti}) \in \mathbb{R}^{6\times6}$ is a diagonal matrix with positive entries $c_{ti} \in \mathbb{R}$ denoting the share of the robot assistance for each degree of freedom. The gain c_{ti} takes values between 0 and 1, where 0 means that only the human applies the required force, and 1 means that the robot performs the task autonomously. To specify $\boldsymbol{h}_{ti}$ from (4.8), we require to find the velocity profile of the ongoing task, $\boldsymbol{v}_t$, that matches the human's velocity $\boldsymbol{v}_h$.

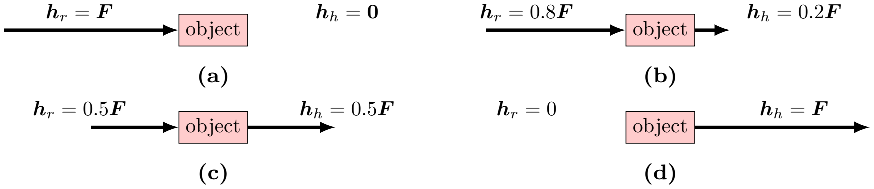
$\boldsymbol{h}_r = \boldsymbol{F}$
object
$\boldsymbol{h}_h = \boldsymbol{0}$
(a)
$\boldsymbol{h}_r = 0.8\boldsymbol{F}$
object
$\boldsymbol{h}_h = 0.2\boldsymbol{F}$
(b)
$\boldsymbol{h}_r = 0.5\boldsymbol{F}$
object
$\boldsymbol{h}_h = 0.5\boldsymbol{F}$
(c)
$\boldsymbol{h}_r = 0$
object
$\boldsymbol{h}_h = \boldsymbol{F}$
(d)

Figure 4.3: In all figures, the object undergoes the same motion. The roles of the robot and the human are different for each case. In (a), the robot moves the object without human assistance. Cases (b) and (c) show a mixed role. In (d), the human moves the object without robot assistance.

4.4 Task adaptation

For the purpose of a generic task definition for object handling, we focus on primitive motions of a rigid-body object. We use Chasles' theorem, which states [71]: "any spatial displacement is a composition of a rotation about some axis and a translation along the same axis." In this regard, we define three local tasks to describe the motion of an object generally. The first task is free motion which has a task velocity of zero. The second task is pure rotation where the object is rotating around a screw axis with an angular velocity, parallel to the angular velocity vector, and a velocity along this axis. The third task is pure translation where the object has a rotational velocity of zero. The task definitions are described in detail in paper C. An example of such tasks for a planar case is presented in Fig. 4.4. The task set can be expanded by other tasks formulated using dynamical systems such as tasks defined in [70]. Khansari *et al.* [70] generate the tasks globally using the dynamical systems. They propose a learning method called Stable Estimator of Dynamical Systems to learn the dynamical system using a set of demonstrations. Unlike [64], [70], the task trajectories proposed in this thesis are defined locally with

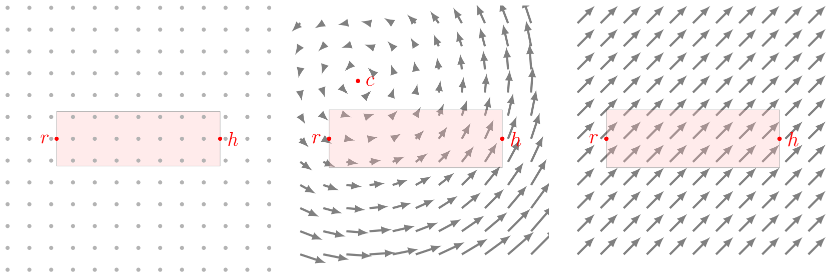

(a) **(b)** **(c)**

Figure 4.4: Velocity profile of a) free motion task, b) rotation task, and c) translation task.

respect to the world frame.

To find the most similar task, we propose to minimize the error between the velocity of the ongoing task and the velocities generated by the pre-defined tasks for the last N_d number of samples. This problem is formulated as a Mixed-Integer Linear Programming (MILP), where the cost function is the linear combination of the state of the tasks b_i, i.e., active or inactive, and the error between the last N_d samples of the velocity of the robot, $\boldsymbol{v}_r$, and the corresponding velocities of all tasks, $\boldsymbol{\mathcal{T}}_i(\boldsymbol{x}_r, t)$.

This is formulated as the following optimization problem:

$$\min_{\boldsymbol{b}} \sum_{i=1:N_t} \left(b_i \sum_{j=1:N_d} \|\boldsymbol{v}_{r_j} - \boldsymbol{\mathcal{T}}_{i,j}(\boldsymbol{x}_r, t)\| \right) \tag{4.9a}$$

$$\text{subj. to} \quad \forall i \in \{1 : N_t\}, b_i \in \{0, 1\} \tag{4.9b}$$

$$\mathbf{1}^T \boldsymbol{b} = 1 \tag{4.9c}$$

$$\forall i \in \{1 : N_t\}, b_i \|\boldsymbol{v}_r - \boldsymbol{\mathcal{T}}_i(\boldsymbol{x}_r, t)\| \leq \check{v}_i \tag{4.9d}$$

$$\forall i \in \{1 : N_t\}, b_i \|\boldsymbol{h}_h - \boldsymbol{h}_{id}\| \leq \check{h}_i \tag{4.9e}$$

where $N_t \in \mathbb{N}$ is the number of tasks, $N_d \in \mathbb{N}$ is the number of collected samples, and $b_i = \{0, 1\}$ decides whether a task is active, i.e., $b_i = 1$. $\boldsymbol{I}$ is the identity matrix, $\boldsymbol{b} = [b_1, \ldots, b_{N_t}]$, $\mathbf{1} \in \mathbb{R}^{N_t}$ is an all-one matrix, $\check{v}_i \in \mathbb{R}$ is the bound on the error of the velocities, and $\check{h}_i$ is the bound on the difference of human applied and desired forces, i.e., $\boldsymbol{h}_h - \boldsymbol{h}_{id}$. Constraint (4.9b) ensures that a task is either inactive or active, i.e., $b_i = 0, 1$. Note that a mixed-task role can be achieved by changing the constraint (4.9b) to "$\forall i \in \{1 : N_t\}, 0 \leq b_i \leq 1$," which converts the optimization problem (4.9) to a convex optimization problem. This may be desirable in the case of a large number of tasks. Constraint (4.9c) ensures that only one task is active at a time. Constraint (4.9d) determines whether the selected task is similar to the current motion. To clarify, this constraint decides whether the error of the velocity for the identified task is within the predefined bound, $\check{v}_i$. Finally, Constraint (4.9e) guarantees that the robot will not perform a task if the human does not apply her/his share of the required force on the object. Should any of the constraints in (4.9) not be met, the free motion task is selected and the human can move the object in all degrees of freedom, independently.

Remark: Formulating the task identification as an optimization problem is a flexible and scalable approach that can accommodate constraints and numerous tasks. Additional specific-purpose tasks that can be learned by dynamical systems [69], [70] can be added along with the current tasks.

In paper C, the proposed task-based control algorithm is evaluated in simulation and experimental studies. In the simulation study, without uncertainties in the modeling and parameters, the human applied force is reduced equally to the preset load-share of the robot when the tasks were identified. In the experimental study, the human effort is reduced proportionally to the preset load-share of the robot, which means that an increase in the robot load share leads to a reduction in the human effort. It should be emphasized that the translation/rotation problem is also avoided by the control design. The studies show that the proposed control algorithm can successfully reduce the human effort in shared human-robot object transportation. The reader is referred to Paper C for more details.

CHAPTER 5

Conclusion and Future Work

This thesis contributes to the field of physical human-robot interaction by investigating the effects of internal time delays on the stability of the system and by addressing the challenges of identifying human haptic commands and responding to them in shared human-robot object handling.

In paper A, we investigate the effect of internal time delay on the stability of a PHRI system for a direct interaction. The internal time delay is modeled with an exponential function, and the stability of the coupled human-robot system is analyzed as a time-delayed system. To evaluate the stability, first the stability of the non-delayed system is evaluated, and then the poles of the characteristic equation are inspected to establish if the imaginary axis is crossed. In the case of poles crossing the imaginary axis, the minimum time delay for which the system is stable, is calculated and used to evaluate stability. We also analyze the effect of backdrivability, first-order filters and admittance controller on the stability of the coupled human-robot system. Since the backdrivable robots are preferable for PHRI, we show that converting a non-backdrivable robot to a backdrivable one using force measurements with time delay requires more caution, especially for interaction with stiff environments. Although we, in Paper A, consider the case of a single time delay in the system, an interesting direction for future study will be to extend the application of the analysis approach for a shared human-robot object manipulation to include additional sources of time delay, e.g., delays in measurement of the object's velocity and acceleration.

Papers B and C explore the topic of shared object handling in physical human-robot interaction. Haptic sensing and analysis of interaction wrenches are crucial for developing effective collaboration between humans and robots. The focus of paper B is on estimating the grasp position of the human for human-robot collaborative object manipulation to enable an accurate calculation of applied human force and overcome the translation/rotation problem. While many studies consider no external torque for contact, in this paper, we explicitly take into account the effect of the human-applied torque to localize the human grasp and evaluate the estimates. The results show that the conventional contact point estimation is not accurate for the generic case of human grasp, and the approach for grasp point estimation proposed in Paper B is more robust and accurate for estimating the human grasp position, especially in the presence of human-applied torque. In paper C, we exploit the known human grasp position to design a control scheme for shared human-robot object handling. We also propose a formulation of three generic tasks to describe the motion of the object. Then, we present an algorithm to find the task most similar to the robot's motion and calculate the desired force of the robot to reduce the force applied by the human. The proposed control scheme is verified through a set of simulation and experimental scenarios and successfully reduces the human applied force for the similar motions. The thesis considers the problems of human grasp position estimation and object handling, separately. The limitation of the control scheme proposed in Paper C is the assumption that the human grasp position is considered as known, which can be alleviated using the method proposed in Paper B. For future studies, an indirect adaptive control scheme where the human grasp position can be provided by the estimator and used as the true grasp position in the control scheme will be investigated. Furthermore, conducting a user study to evaluate the performance of the proposed control scheme is a top priority. In addition to performance metrics, quantitative and qualitative results from different users interacting with the robot will be collected and analyzed. Another interesting idea for future work is to augment the task adaptation algorithm with force measurements and extend the proposed control for tasks that involve contact with a surface, such as assembly [72], polishing [73], and food-cutting [74].

References

[1] "Robots and robotic devices — Collaborative robots," International Organization for Standardization, Geneva, Standard ISO/TS 15066:2016, 2016.

[2] V. Villani, F. Pini, F. Leali, and C. Secchi, "Survey on human–robot collaboration in industrial settings: Safety, intuitive interfaces and applications," *Mechatronics*, vol. 55, pp. 248–266, 2018.

[3] G. Michalos, S. Makris, J. Spiliotopoulos, I. Misios, P. Tsarouchi, and G. Chryssolouris, "Robo-partner: Seamless human-robot cooperation for intelligent, flexible and safe operations in the assembly factories of the future," *Procedia CIRP*, vol. 23, pp. 71–76, 2014.

[4] R. R. Murphy, D. Riddle, and E. Rasmussen, "Robot-assisted medical reachback: A survey of how medical personnel expect to interact with rescue robots," in *IEEE International Workshop on Robot and Human Interactive Communication (RO-MAN)*, 2004, pp. 301–306.

[5] W. Bluethmann, R. Ambrose, M. Diftler, S. Askew, E. Huber, M. Goza, F. Rehnmark, C. Lovchik, and D. Magruder, "Robonaut: A robot designed to work with humans in space," *Autonomous robots*, vol. 14, no. 2-3, pp. 179–197, 2003.

[6] J. Pineau, M. Montemerlo, M. Pollack, N. Roy, and S. Thrun, "Towards robotic assistants in nursing homes: Challenges and results," *Robotics and autonomous systems*, vol. 42, no. 3-4, pp. 271–281, 2003.

[7] A. Sharma. (2019). “The future of collaborative robots,” [Online]. Available: `https://www.interactanalysis.com/collaborative-robots/`.

[8] LKH PRECICON Pte Ltd. (2021). “Making operations safer with cobot in the covid19 era,” [Online]. Available: `https://www.precicon.com.sg/industry_4_0/making-operations-safer-with-cobot-in-the-covid19-era`.

[9] CleanEnviro Summit Singapore (CESG). (2021). “Working with cobots to fight covid-19,” [Online]. Available: `https://www.cleanenvirosummit.gov.sg/docs/default-source/default-document-library/resources/publications/edm/2021_0301_cesg-catalyst-will-be-back-this-year.pdf`.

[10] R. K. Singh. (2021). “Coronavirus pandemic advances the march of ’cobots’,” [Online]. Available: `https://www.reuters.com/article/us-health-coronavirus-automation-idUSKCN24L18T`.

[11] M. A. Goodrich, A. C. Schultz, *et al.*, “Human–robot interaction: A survey,” *Foundations and Trends® in Human–Computer Interaction*, vol. 1, no. 3, pp. 203–275, 2008.

[12] T. B. Sheridan, “Human–robot interaction: Status and challenges,” *Human factors*, vol. 58, no. 4, pp. 525–532, 2016.

[13] D. J. Agravante, A. Cherubini, A. Bussy, P. Gergondet, and A. Kheddar, “Collaborative human-humanoid carrying using vision and haptic sensing,” in *IEEE International Conference on Robotics and Automation (ICRA)*, 2014, pp. 607–612.

[14] D. P. Losey, C. G. McDonald, E. Battaglia, and M. K. O’Malley, “A review of intent detection, arbitration, and communication aspects of shared control for physical human–robot interaction,” *Applied Mechanics Reviews*, vol. 70, no. 1, p. 010 804, 2018.

[15] A. Ajoudani, A. M. Zanchettin, S. Ivaldi, A. Albu-Schäffer, K. Kosuge, and O. Khatib, “Progress and prospects of the human–robot collaboration,” *Autonomous Robots*, pp. 1–19, 2018.

[16] X. Yu, W. He, Q. Li, Y. Li, and B. Li, “Human-robot co-carrying using visual and force sensing,” *IEEE Transactions on Industrial Electronics*, 2020.

[17] J. R. Medina, M. Shelley, D. Lee, W. Takano, and S. Hirche, "Towards interactive physical robotic assistance: Parameterizing motion primitives through natural language," in *IEEE International Symposium on Robot and Human Interactive Communication (RO-MAN)*, 2012, pp. 1097–1102.

[18] D. Sirintuna, I. Ozdamar, Y. Aydin, and C. Basdogan, "Detecting human motion intention during phri using artificial neural networks trained by emg signals," in *IEEE International Symposium on Robot and Human Interactive Communication (RO-MAN)*, 2020, pp. 1280–1287.

[19] K. Li, J. Zhang, L. Wang, M. Zhang, J. Li, and S. Bao, "A review of the key technologies for semg-based human-robot interaction systems," *Biomedical Signal Processing and Control*, vol. 62, p. 102 074, 2020.

[20] V. Hayward and O. R. Astley, "Performance measures for haptic interfaces," in *Robotics research*, Springer, 1996, pp. 195–206.

[21] A. Mörtl, M. Lawitzky, A. Kucukyilmaz, M. Sezgin, C. Basdogan, and S. Hirche, "The role of roles: Physical cooperation between humans and robots," *The International Journal of Robotics Research*, vol. 31, no. 13, pp. 1656–1674, 2012.

[22] J. Dumora, F. Geffard, C. Bidard, T. Brouillet, and P. Fraisse, "Experimental study on haptic communication of a human in a shared human-robot collaborative task," in *IEEE/RSJ International Conference on Intelligent Robots and Systems (IROS)*, 2012, pp. 5137–5144.

[23] Y. Karayiannidis, C. Smith, and D. Kragic, "Mapping human intentions to robot motions via physical interaction through a jointly-held object," in *IEEE International Symposium on Robot and Human Interactive Communication (RO-MAN)*, 2014, pp. 391–397.

[24] A. Kucukyilmaz, T. M. Sezgin, and C. Basdogan, "Intention recognition for dynamic role exchange in haptic collaboration," *IEEE transactions on haptics*, vol. 6, no. 1, pp. 58–68, 2013.

[25] C. E. Madan, A. Kucukyilmaz, T. M. Sezgin, and C. Basdogan, "Recognition of haptic interaction patterns in dyadic joint object manipulation," *IEEE transactions on haptics*, vol. 8, no. 1, pp. 54–66, 2014.

[26] E. Noohi, M. Žefran, and J. L. Patton, “A model for human–human collaborative object manipulation and its application to human–robot interaction,” *IEEE transactions on robotics*, vol. 32, no. 4, pp. 880–896, 2016.

[27] E. Noohi and M. Žefran, “Estimating human intention during a human–robot cooperative task based on the internal force internal force model,” *Trends in Control and Decision-Making for Human–Robot Collaboration Systems*, pp. 83–109, 2017.

[28] L. Sanneman, C. Fourie, and J. A. Shah, “The state of industrial robotics: Emerging technologies, challenges, and key research directions,” *arXiv preprint arXiv:2010.14537*, 2020.

[29] D. Lee and M. W. Spong, “Passive bilateral teleoperation with constant time delay,” *IEEE transactions on robotics*, vol. 22, no. 2, pp. 269–281, 2006.

[30] D. Lee, “Extension of colgate’s passivity condition for variable-rate haptics,” in *IEEE/RSJ International Conference on Intelligent Robots and Systems (IROS)*, 2009, pp. 1761–1766.

[31] V. Duchaine and C. M. Gosselin, “Investigation of human-robot interaction stability using lyapunov theory,” in *IEEE International Conference on Robotics and Automation (ICRA)*, 2008, pp. 2189–2194.

[32] J. E. Colgate and G. G. Schenkel, “Passivity of a class of sampled-data systems: Application to haptic interfaces,” *Journal of robotic systems*, vol. 14, no. 1, pp. 37–47, 1997.

[33] H. K. Khalil and J. W. Grizzle, *Nonlinear systems.* Upper Saddle River, NJ: Prentice hall, 2002, vol. 3.

[34] R. J. Ansari, M. Zareinejad, S. Rezaei, K. Baghestan, and N. Sarli, “Stable multi-user interaction with cooperative haptic virtual environments by a modification of passive set-position modulation,” *IET Control Theory & Applications*, vol. 6, no. 16, pp. 2538–2548, 2012.

[35] K. H. Lee, S. G. Baek, H. J. Lee, H. R. Choi, H. Moon, and J. C. Koo, “Enhanced transparency for physical human-robot interaction using human hand impedance compensation,” *IEEE/ASME Transactions on Mechatronics*, vol. 23, no. 6, pp. 2662–2670, 2018.

[36] F. Müller, J. Jäkel, J. Suchý, and U. Thomas, "Stability of nonlinear time-delay systems describing human–robot interaction," *IEEE/ASME Transactions on Mechatronics*, vol. 24, no. 6, pp. 2696–2705, 2019.

[37] F. Dimeas and N. Aspragathos, "Online stability in human-robot cooperation with admittance control," *IEEE transactions on haptics*, vol. 9, no. 2, pp. 267–278, 2016.

[38] D. Ryu, J.-B. Song, S. Kang, and M. Kim, "Frequency domain stability observer and active damping control for stable haptic interaction," *IET Control Theory & Applications*, vol. 2, no. 4, pp. 261–268, 2008.

[39] O. Egeland and J. T. Gravdahl, *Modeling and Simulation for Automatic Control.* Trondheim, Norway: Marine Cybernetics AS, 2002.

[40] A. Q. Keemink, H. van der Kooij, and A. H. Stienen, "Admittance control for physical human–robot interaction," *The International Journal of Robotics Research*, vol. 37, no. 11, pp. 1421–1444, 2018.

[41] C. Ott, R. Mukherjee, and Y. Nakamura, "Unified impedance and admittance control," in *IEEE International Conference on Robotics and Automation (ICRA)*, 2010, pp. 554–561.

[42] S. P. Buerger and N. Hogan, "Complementary stability and loop shaping for improved human–robot interaction," *IEEE Transactions on Robotics*, vol. 23, no. 2, pp. 232–244, 2007.

[43] B. Brogliato, R. Lozano, B. Maschke, and O. Egeland, *Dissipative systems analysis and control: Theory and Applications.* London, UK: Springer Science and Business Media, 2007.

[44] E. Fridman, *Introduction to time-delay systems: Analysis and control.* New York: Springer, 2014.

[45] J. E. Marshall, *Time-delay systems: stability and performance criteria with applications.* Upper Saddle River, NJ: Prentice Hall, 1992.

[46] J. R. Partington, C. Series, *et al.*, *Linear operators and linear systems: an analytical approach to control theory.* Cambridge, UK: Cambridge University Press, 2004, vol. 60.

[47] K. Gu, J. Chen, and V. L. Kharitonov, *Stability of time-delay systems.* New York: Springer Science & Business Media, 2003.

[48] M. S. Erden and A. Billard, “End-point impedance measurements across dominant and nondominant hands and robotic assistance with directional damping,” *IEEE transactions on cybernetics*, vol. 45, no. 6, pp. 1146–1157, 2014.

[49] T. Takubo, H. Arai, Y. Hayashibara, and K. Tanie, “Human-robot cooperative manipulation using a virtual nonholonomic constraint,” *The International Journal of Robotics Research*, vol. 21, no. 5-6, pp. 541–553, 2002.

[50] R. J. Ansari and Y. Karayiannidis, “Reducing the human effort for human-robot cooperative object manipulation via control design,” *IFAC-PapersOnLine*, vol. 50, no. 1, pp. 14 922–14 927, 2017.

[51] Y. Karayiannidis, C. Smith, F. E. Vina, and D. Kragic, “Online kinematics estimation for active human-robot manipulation of jointly held objects,” in *IEEE/RSJ International Conference on Intelligent Robots and Systems (IROS)*, 2013, pp. 4872–4878.

[52] Y. Karayiannidis, C. Smith, F. E. Viña, and D. Kragic, “Online contact point estimation for uncalibrated tool use,” in *IEEE International Conference on Robotics and Automation (ICRA)*, 2014, pp. 2488–2494.

[53] L. Manuelli and R. Tedrake, “Localizing external contact using proprioceptive sensors: The contact particle filter,” in *IEEE/RSJ International Conference on Intelligent Robots and Systems (IROS)*, 2016, pp. 5062–5069.

[54] N. Fazeli, R. Kolbert, R. Tedrake, and A. Rodriguez, “Parameter and contact force estimation of planar rigid-bodies undergoing frictional contact,” *The International Journal of Robotics Research*, vol. 36, no. 13-14, pp. 1437–1454, 2017.

[55] S. Haddadin, A. De Luca, and A. Albu-Schäffer, “Robot collisions: A survey on detection, isolation, and identification,” *IEEE Transactions on Robotics*, vol. 33, no. 6, pp. 1292–1312, 2017.

[56] M. Kollmitz, D. Büscher, T. Schubert, and W. Burgard, “Whole-body sensory concept for compliant mobile robots,” in *IEEE International Conference on Robotics and Automation (ICRA)*, 2018, pp. 5429–5435.

[57] A. Zwiener, C. Geckeler, and A. Zell, “Contact point localization for articulated manipulators with proprioceptive sensors and machine learning,” in *IEEE International Conference on Robotics and Automation (ICRA)*, 2018, pp. 323–329.

[58] Y. J. Heo, D. Kim, W. Lee, H. Kim, J. Park, and W. K. Chung, “Collision detection for industrial collaborative robots: A deep learning approach,” *IEEE Robotics and Automation Letters*, vol. 4, no. 2, pp. 740–746, 2019.

[59] D. Ćehajić, S. Erhart, and S. Hirche, “Grasp pose estimation in human-robot manipulation tasks using wearable motion sensors,” in *IEEE/RSJ International Conference on Intelligent Robots and Systems (IROS)*, 2015, pp. 1031–1036.

[60] Y. Karayiannidis and Z. Doulgeri, “Adaptive control of robot contact tasks with on-line learning of planar surfaces,” *Automatica*, vol. 45, no. 10, pp. 2374–2382, 2009.

[61] J. L. Meriam and L. G. Kraige, *Engineering mechanics: dynamics.* Danvers, MA: John Wiley & Sons, 2012, vol. 2.

[62] D. Ćehajić, P. B. g. Dohmann, and S. Hirche, “Estimating unknown object dynamics in human-robot manipulation tasks,” in *IEEE International Conference on Robotics and Automation (ICRA)*, 2017, pp. 1730–1737.

[63] L. Ljung, “System identification,” in *Signal analysis and prediction*, Springer, 1998, pp. 163–173.

[64] M. Khoramshahi and A. Billard, “A dynamical system approach to task-adaptation in physical human–robot interaction,” *Autonomous Robots*, vol. 43, no. 4, pp. 927–946, 2019.

[65] S. Hayati, “Hybrid position/force control of multi-arm cooperating robots,” in *IEEE International Conference on Robotics and Automation (ICRA)*, vol. 3, 1986, pp. 82–89.

[66] O. Khatib, “Object manipulation in a multi-effector robot system,” in *Proceedings of the 4th international symposium on Robotics Research*, MIT Press, 1988, pp. 137–144.

[67] C. Smith, Y. Karayiannidis, L. Nalpantidis, X. Gratal, P. Qi, D. V. Dimarogonas, and D. Kragic, “Dual arm manipulation—a survey,” *Robotics and Autonomous systems*, vol. 60, no. 10, pp. 1340–1353, 2012.

[68] S. Erhart and S. Hirche, “Model and analysis of the interaction dynamics in cooperative manipulation tasks,” *IEEE Transactions on Robotics*, vol. 32, no. 3, pp. 672–683, 2016.

[69] A. Dahlin and Y. Karayiannidis, “Adaptive trajectory generation under velocity constraints using dynamical movement primitives,” *IEEE Control Systems Letters*, vol. 4, no. 2, pp. 438–443, 2019.

[70] S. M. Khansari-Zadeh and A. Billard, “Learning stable nonlinear dynamical systems with gaussian mixture models,” *IEEE Transactions on Robotics*, vol. 27, no. 5, pp. 943–957, 2011.

[71] M. T. Mason, *Mechanics of robotic manipulation.* Cambridge, MA: MIT press, 2001.

[72] A. Salem and Y. Karayiannidis, “Robotic assembly of rounded parts with and without threads,” *IEEE Robotics and Automation Letters*, vol. 5, no. 2, pp. 2467–2474, 2020.

[73] S. S. M. Salehian and A. Billard, “A dynamical-system-based approach for controlling robotic manipulators during noncontact/contact transitions,” *IEEE Robotics and Automation Letters*, vol. 3, no. 4, pp. 2738–2745, 2018.

[74] I. Mitsioni, Y. Karayiannidis, and D. Kragic, “Modelling and learning dynamics for robotic food-cutting,” *arXiv preprint arXiv:2003.09179*, 2020.

Part II

Included Papers